

Theoretical study of $R_{1\rho}$ rotating-frame and R_2 free-precession relaxation in the presence of n -site chemical exchange

Oleg Trott and Arthur G. Palmer III*

Department of Biochemistry and Molecular Biophysics, Columbia University, 630 West 168th Street, New York, NY 10032, USA

Received 13 March 2004; revised 10 June 2004

Available online 6 July 2004

Abstract

The n -site Bloch–McConnell equations describe the evolution of nuclear spin magnetization in the laboratory or rotating frames of reference for molecules subject to chemical or conformational interconversions between n species with distinct NMR chemical shifts. Perturbation theory is used to approximate the largest eigenvalue of the Bloch–McConnell equations and obtain analytical expressions for the rotating-frame relaxation rate constant and for the laboratory frame resonance frequency and transverse relaxation rate constant. The perturbation treatment is valid whenever the population of one site is dominant. The new results are generally applicable to investigations of kinetic processes by NMR spectroscopy.

© 2004 Elsevier Inc. All rights reserved.

Keywords: Chemical exchange; Asymmetric populations; Rotating-frame relaxation

1. Introduction

Chemical reaction kinetics can be quantified using a variety of techniques in nuclear magnetic resonance (NMR) spectroscopy [1]. Chemical exchange relaxation or line broadening results from stochastic transitions between chemical or conformational states with different magnetic properties. As a consequence, nuclear spin coherences are dephased, causing an increase in phenomenological relaxation rate constants. Chemical exchange phenomena contribute to both R_2 , the free-precession relaxation rate constant for transverse magnetization, and $R_{1\rho}$, the characteristic relaxation rate constant for magnetization spin-locked along the direction of the effective magnetic field in the rotating frame of reference. The dependence of $R_{1\rho}$ upon on the amplitude and frequency of the applied rf field is called relaxation dispersion. $R_{1\rho}$ rotating-frame relaxation experiments provide a powerful means to elucidate intramolecular conformational changes, ligand binding, and folding of proteins and other biological macromolecules that occur with rate constants between 10^1 and 10^5 s⁻¹ [1].

In experimental studies, $R_{1\rho}$ relaxation dispersion data are analyzed using theoretical expressions derived for particular chemical exchange mechanisms to determine the rate constants, site populations, and resonance frequencies for nuclear spins affected by the kinetic process. For applications to slowly tumbling macromolecules with complex NMR spectra, expressions are needed that incorporate the conditions $R_2 > R_1$ and off-resonance rf fields. When exchange is fast compared to the differences in resonance frequencies for spins in different sites, a Redfield perturbation approach can be used to derive theoretical expressions for $R_{1\rho}$ [2,3]. When exchange is not fast, approximate theoretical expressions for $R_{1\rho}$ can be obtained by both time-domain and frequency-domain analyses of the stochastic Liouville equation or the Bloch–McConnell equation [3–5]. Theoretical results have been reported for a number of cases: fast 2-site exchange [2,6], fast n -site exchange [3], and 2-site exchange outside of the fast exchange limit under the condition that the site populations are asymmetric [4,5].

Although most experimental studies of chemical exchange in proteins using $R_{1\rho}$ relaxation dispersion have assumed fast 2-site exchange [1], a recent investigation has shown improved results when using more general expressions for 2-site exchange appropriate for all time

* Corresponding author. Fax: 1-212-305-6949.

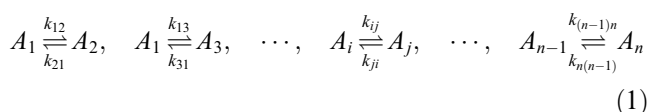
E-mail address: agp6@columbia.edu (A.G. Palmer III).

scales [7]. Furthermore, experimental identification of 3-site exchange processes in proteins underlines the importance of improved theoretical approaches for describing n -site exchange phenomena in NMR spectroscopy [8–10].

The present paper generalizes the approach of Trott and Palmer [4] from 2-site to n -site chemical exchange processes. The resulting expressions for $R_{1\rho}$ are accurate for all exchange time scales provided that the population of one site is dominant. The same formalism is used to analyze n -site chemical exchange contributions to free-precession evolution in the absence of rf fields. The resulting expressions extend the Swift–Connick relationships [11].

2. Bloch–McConnell equation

We consider a chemical reaction or conformational transition that exchanges a nuclear spin between n sites A_i with distinct magnetic environments,



in which k_{ij} is the reaction rate constant for the transition from i th to j th site. The chemical kinetics of such a system are described by the equation:

$$\frac{d}{dt} \vec{c} = \mathbf{K} \vec{c}, \quad (2)$$

in which the kinetics matrix is given by:

$$\mathbf{K} = \begin{pmatrix} -s_1 & k_{21} & \cdots & k_{n1} \\ k_{12} & -s_2 & \cdots & k_{n2} \\ \vdots & \vdots & \ddots & \vdots \\ k_{1n} & k_{2n} & \cdots & -s_n \end{pmatrix}, \quad (3)$$

$$\mathbf{K}_{ii} = -s_i = -\sum_{\substack{j=1 \\ j \neq i}}^n k_{ij}, \quad (4)$$

$\mathbf{K}_{ij} = k_{ji}$ for $i \neq j$, and the elements of \vec{c} are the site populations of the reacting species. The equilibrium site populations are defined by $\mathbf{K} \vec{c} = 0$. In the absence of exchange processes, the time evolution of the nuclear spin magnetization of the i th site is given by the Bloch equation [12]:

$$\frac{d}{dt} \vec{M}_i = \mathbf{L}_i \vec{M}_i + R_{1i} \vec{M}_{0i}, \quad (5)$$

in which

$$\mathbf{L}_i = \begin{pmatrix} -R_{2i} & -\delta_i & 0 \\ \delta_i & -R_{2i} & -\omega \\ 0 & \omega & -R_{1i} \end{pmatrix}; \quad (6)$$

the resonance offset for the i th site in the rotating frame is defined as

$$\delta_i = \Omega_i - \omega_{\text{rf}}, \quad (7)$$

where Ω_i is the resonance frequency of the i th site; ω_{rf} is the frequency and ω is the amplitude, defined by the Rabi frequency, of the applied rf field; R_{1i} and R_{2i} are the intrinsic longitudinal and transverse relaxation rates, respectively, resulting from processes other than chemical exchange; $\vec{M}_i = (M_{xi}, M_{yi}, M_{zi})^T$ is the three-dimensional Cartesian magnetization vector; and $\vec{M}_{0i} = (0, 0, M_{0i})^T$ is the time-independent thermal equilibrium magnetization in the absence of the rf field [12].

The state of the n -site system, presented in Eq. (1), is described by a $3n$ -dimensional magnetization vector

$$\vec{M} = \begin{pmatrix} \vec{M}_1 \\ \vec{M}_2 \\ \vdots \\ \vec{M}_n \end{pmatrix}. \quad (8)$$

Its time evolution is a superposition of the precession-relaxation of Eq. (5) and the exchange processes of Eq. (2) and is given by the Bloch–McConnell equation [13]:

$$\frac{d}{dt} \vec{M} = \mathbf{D} \vec{M} + \vec{B}, \quad (9)$$

where

$$\mathbf{D} = \mathbf{L} + \mathbf{K} \otimes \mathbf{1}_s, \quad (10)$$

$$\mathbf{L} = \oplus_{i=1}^n \mathbf{L}_i = \begin{pmatrix} \mathbf{L}_1 & & & \\ & \mathbf{L}_2 & & \\ & & \ddots & \\ & & & \mathbf{L}_n \end{pmatrix}, \quad (11)$$

$$\vec{B} = \begin{pmatrix} R_{11} \vec{M}_{01} \\ R_{12} \vec{M}_{02} \\ \vdots \\ R_{1n} \vec{M}_{0n} \end{pmatrix}, \quad (12)$$

where $\mathbf{1}_s$ is the identity matrix in the spin space, i.e., the 3×3 identity matrix, and \otimes and \oplus denote the direct product and sum, respectively.

In general, Eq. (9) is a first-order linear differential equation with constant coefficients. Its solution has the form

$$\vec{M}(t) = \sum_{i=1}^{3n} e^{\lambda_i t} \vec{l}_i + \vec{a}, \quad (13)$$

where λ_i is the i th eigenvalue of the matrix \mathbf{D} in Eq. (10), \vec{l}_i is proportional to the corresponding eigenvector, and \vec{a} is the stationary solution.

The eigenvalues of a real matrix are the roots of the corresponding characteristic polynomial, which is also

necessarily a real function. Therefore, the set of eigenvalues consists of m real values and $(3n - m)/2$ conjugate pairs of complex values, in which $m \leq n$. For realistic experimental conditions, numerical simulations establish that $m = n$ and that the matrix \mathbf{D} has n real eigenvalues and n pairs of complex ones with relatively large imaginary parts. In practice, ω varies at different points within the macroscopic NMR sample due to instrumental imperfections. The ω inhomogeneity introduces variability in the eigenvalues and in the orientation of the eigenbasis. While the latter effect is insignificant, eigenvalue inhomogeneity results in rapid, on the time scale of the variation the ω due to the inhomogeneity or faster, averaging of the oscillatory (i.e., corresponding to non-real eigenvalues) components to zero. In many cases of interest, one real eigenvalue is significantly greater than the other $n - 1$ ones. On experimentally accessible time scales, the largest (least negative) real eigenvalue dominates the evolution of the magnetization components and the relaxation decay is essentially monoexponential. Thus, the problem of finding the relaxation rate constant $R_{1\rho}$ reduces to finding the largest real eigenvalue λ of the matrix $\mathbf{D} = \mathbf{L} + \mathbf{K} \otimes \mathbf{1}_s$:

$$R_{1\rho} = -\lambda. \quad (14)$$

3. One dominant site

In many systems of practical interest, the free energy difference between some sites is greater than $k_B T$; consequently, the site populations are unequal because even small differences in energy translate into large population differences through the Boltzmann equation.

We consider the case for which the the population of the first site is much greater than the populations of others: $p_1 \gg p_2, \dots, p_n$. Through the detailed balance relationship, this assumption implies that the first column of \mathbf{K} is much smaller than the rest of the matrix, specifically its first row. By \mathbf{K}' , we shall denote the matrix obtained from \mathbf{K} by setting its first column to zero. Additionally, R_{1i} and R_{2i} are assumed to be much smaller than other non-trivial components of \mathbf{L}_i . The latter assumption is not essential to the approach to be presented (vide infra), but simplifies the resulting expressions. We also introduce an approximation of \mathbf{L}_i

$$\mathbf{L}'_i = \begin{pmatrix} 0 & -\delta_i & 0 \\ \delta_i & 0 & -\omega \\ 0 & \omega & 0 \end{pmatrix}. \quad (15)$$

Therefore, we can compute the the largest real eigenvalue λ of the matrix $\mathbf{D} = \mathbf{L} + \mathbf{K} \otimes \mathbf{1}_s$ as a perturbed

value of the largest real eigenvalue λ' of the matrix $\mathbf{D}' = \mathbf{L}' + \mathbf{K}' \otimes \mathbf{1}_s$, where $\mathbf{L}' = \bigoplus_{i=1}^n \mathbf{L}'_i$. Examination of \mathbf{D}' , shows that the eigenvalue λ' is zero, and the corresponding right eigenvector is

$$\vec{x} = \begin{pmatrix} \vec{v} \\ \vec{0} \\ \vdots \\ \vec{0} \end{pmatrix}, \quad (16)$$

in which \vec{v} is both left and right eigenvector of \mathbf{L}'_1 corresponding to its zero eigenvalue:

$$\vec{v} = \frac{1}{\omega_{e1}} \begin{pmatrix} \omega \\ 0 \\ \delta_1 \end{pmatrix}, \quad (17)$$

and

$$\omega_{ei} = \sqrt{\delta_i^2 + \omega^2}. \quad (18)$$

The first three elements of the corresponding left eigenvector \vec{y} of \mathbf{D}' are also \vec{v} . Therefore, the eigenvector can be looked for in the form

$$\vec{y} = \begin{pmatrix} \vec{v} \\ \vec{v} \\ \vdots \\ \vec{v} \end{pmatrix} - \begin{pmatrix} \vec{0} \\ \vec{z}_2 \\ \vdots \\ \vec{z}_n \end{pmatrix}. \quad (19)$$

From perturbation theory [14],

$$\lambda = \lambda' + \frac{\vec{y}^T (\mathbf{D} - \mathbf{D}') \vec{x}}{\vec{y}^T \vec{x}}. \quad (20)$$

Using the facts that $\lambda' = 0$, $\vec{y}^T \vec{x} = 1$, and

$$\vec{y}^T (\mathbf{L} - \mathbf{L}') \vec{x} = \vec{v}^T (\mathbf{L}_1 - \mathbf{L}'_1) \vec{v} \quad (21)$$

$$= -\frac{\delta_1^2}{\omega_{e1}^2} R_{11} - \frac{\omega^2}{\omega_{e1}^2} R_{21}, \quad (22)$$

yields:

$$\lambda = -\frac{\delta_1^2}{\omega_{e1}^2} R_{11} - \frac{\omega^2}{\omega_{e1}^2} R_{21} + \vec{y}^T ((\mathbf{K} - \mathbf{K}') \otimes \mathbf{1}_s) \vec{x}. \quad (23)$$

Using Eq. (19) and the fact that only the first column of $\mathbf{K} - \mathbf{K}'$ is non-zero, we obtain the following expression for λ :

$$\lambda = -\frac{\delta_1^2}{\omega_{e1}^2} R_{11} - \frac{\omega^2}{\omega_{e1}^2} R_{21} - \sum_{i=2}^n k_{1i} \vec{z}_i^T \vec{v}. \quad (24)$$

The values \vec{z}_i are found by substituting Eq. (19) into the definition of the left eigenvector $\vec{y}^T \mathbf{D}' = \lambda' \vec{y}^T = 0$. Transposing and simplifying the resulting expressions, and noting that $\mathbf{L}_i'^T = -\mathbf{L}'_i$, the following equation for the \vec{z}_i values is obtained:

$$\begin{pmatrix} s_2 + \mathbf{L}'_2 & -k_{23} & \cdots & -k_{2n} \\ -k_{32} & s_3 + \mathbf{L}'_3 & \cdots & -k_{3n} \\ \vdots & \vdots & \ddots & \vdots \\ -k_{n2} & -k_{n3} & \cdots & s_n + \mathbf{L}'_n \end{pmatrix} \begin{pmatrix} \bar{z}_2 \\ \bar{z}_3 \\ \vdots \\ \bar{z}_n \end{pmatrix} = \begin{pmatrix} \mathbf{L}'_2 \vec{v} \\ \mathbf{L}'_3 \vec{v} \\ \vdots \\ \mathbf{L}'_n \vec{v} \end{pmatrix}. \quad (25)$$

Eq. (25) is linear, so it can be solved *symbolically* (and automatically) for any n to give the result:

$$R_{1\rho} = \cos^2 \theta_1 R_{11} + \sin^2 \theta_1 R_{21} + \sum_{i=2}^n k_{1i} \bar{z}_i^T \vec{v}, \quad (26)$$

where $\sin \theta_1 = \omega/\omega_{e1}$ and $\cos \theta_1 = \delta_1/\omega_{e1}$. Eq. (26) is one of the primary results of this paper.

For convenience, we also define the effective chemical exchange contribution to relaxation as:

$$R_{\text{ex}} = R_{1\rho}/\sin^2 \theta_1 - R_{11}/\tan^2 \theta_1 - R_{21}. \quad (27)$$

From Eqs. (15) and (17), we note (for use in the following) that:

$$\begin{aligned} (\mathbf{L}'_i + s_i)^{-1} &= \begin{pmatrix} s_i & -\delta_i & 0 \\ \delta_i & s_i & -\omega \\ 0 & \omega & s_i \end{pmatrix}^{-1} = \frac{1}{s_i} \frac{1}{s_i^2 + \omega_{ei}^2} \\ &\times \begin{pmatrix} s_i^2 + \omega^2 & s_i \delta_i & \delta_i \omega \\ -s_i \delta_i & s_i^2 & s_i \omega \\ \delta_i \omega & -s_i \omega & s_i^2 + \delta_i^2 \end{pmatrix} \end{aligned} \quad (28)$$

and

$$\mathbf{L}'_i \vec{v} = \frac{\omega \Delta \omega_{i1}}{\omega_{e1}} \begin{pmatrix} 0 \\ 1 \\ 0 \end{pmatrix} \quad (29)$$

in which $\Delta \omega_{ij} = \delta_i - \delta_j$. We also define:

$$\bar{z}'_i = (\mathbf{L}'_i + s_i)^{-1} \mathbf{L}'_i \vec{v} = \frac{\omega}{\omega_{e1}} \frac{\Delta \omega_{i1}}{s_i^2 + \omega_{ei}^2} \begin{pmatrix} \delta_i \\ s_i \\ -\omega \end{pmatrix}. \quad (30)$$

The following sections consider some special cases of practical interest.

3.1. No minor exchange

We refer to the set of all of the exchange reactions that do not involve the dominant site (site 1) as minor exchange. From Eq. (25), in the absence of the minor exchange, $\bar{z}_i = \bar{z}'_i$. Using this result with the understanding that $s_i = k_{i1}$, we obtain:

$$R_{1\rho} = \cos^2 \theta_1 R_{11} + \sin^2 \theta_1 R_{21} + \sin^2 \theta_1 \sum_{i=2}^n \frac{k_{1i} \Delta \omega_{i1}^2}{k_{i1}^2 + \omega_{ei}^2}. \quad (31)$$

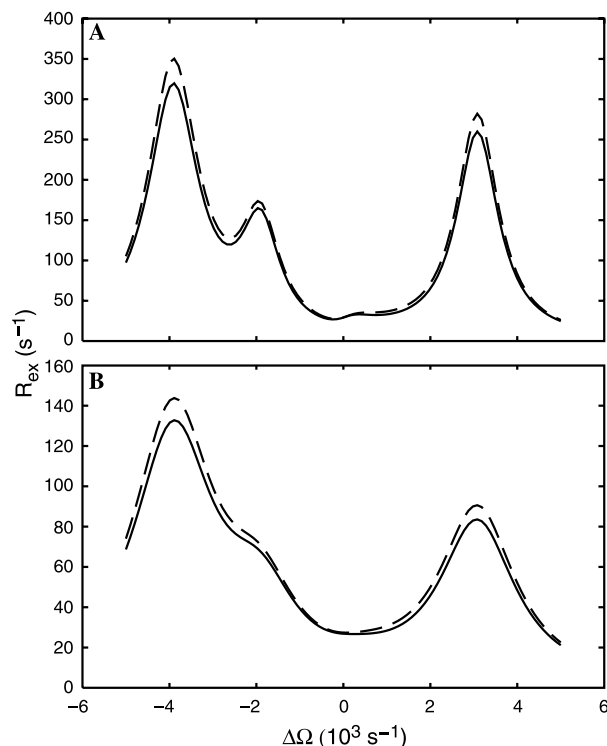


Fig. 1. Offset dependence of R_{ex} for a system with no minor exchange. The solid line represents the exact numerical solution and the dashed line shows the approximate solution obtained from Eq. (31). Curves were calculated using (A) $\omega = 500 \text{ s}^{-1}$ and (B) $\omega = 1000 \text{ s}^{-1}$. Other parameters used in the calculations were: $p_1 = 0.90$, $p_2 = 0.05$, $p_3 = 0.03$, $p_4 = 0.02$, $\delta_2 - \delta_1 = 2000 \text{ s}^{-1}$, $\delta_3 - \delta_1 = -3000 \text{ s}^{-1}$, $\delta_4 - \delta_1 = 000 \text{ s}^{-1}$, $k_{12} + k_{21} = 200 \text{ s}^{-1}$, $k_{13} + k_{31} = 200 \text{ s}^{-1}$, $k_{14} + k_{41} = 4200 \text{ s}^{-1}$, $R_1 = 1.5 \text{ s}^{-1}$, and $R_2 = 11 \text{ s}^{-1}$. The abscissa $\Delta \Omega$ indicates the difference between ω_{rf} and the population-average resonance frequency.

This result generalizes the expression previously reported by Trott and Palmer [4] for 2-site exchange. Fig. 1 illustrates this expression for a 4-site exchange process. The important qualitative result is that the graph of R_{ex} versus resonance offset consists of $n - 1$ Lorentzian-shaped peaks with local maxima occurring when $\delta_i = 0$ for $i = 2, \dots, n$. The i th Lorentzian has a full-width-at-half-height equal to $2(k_{i1}^2 + \omega^2)^{1/2}$. Consequently, the number of components in the R_{ex} profile is most easily discerned when ω is weak, as indicated by comparison of Figs. 1A and 1B.

3.2. Weak minor exchange

We shall call the minor exchange weak, if the rate of conversion from every minor site to the dominant site is much greater than the rates of conversion between minor sites, i.e.,

$$k_{i1} \gg k_{ij}, \quad \text{where } i, j = 2, \dots, n. \quad (32)$$

Multiplying Eq. (25) from the left by $\oplus_{i=2}^n (\mathbf{L}'_i + s_i)^{-1}$, we obtain:

$$\begin{pmatrix} \mathbf{1}_s & -k_{23}(\mathbf{L}'_2 + s_2)^{-1} & \cdots & -k_{2n}(\mathbf{L}'_2 + s_2)^{-1} \\ -k_{32}(\mathbf{L}'_3 + s_3)^{-1} & \mathbf{1}_s & \cdots & -k_{3n}(\mathbf{L}'_3 + s_3)^{-1} \\ \vdots & \vdots & \ddots & \vdots \\ -k_{n2}(\mathbf{L}'_n + s_n)^{-1} & -k_{n3}(\mathbf{L}'_n + s_n)^{-1} & \cdots & \mathbf{1}_s \end{pmatrix} \times \begin{pmatrix} \bar{z}'_2 \\ \bar{z}'_3 \\ \vdots \\ \bar{z}'_n \end{pmatrix} = \begin{pmatrix} \bar{z}'_2 \\ \bar{z}'_3 \\ \vdots \\ \bar{z}'_n \end{pmatrix}. \quad (33)$$

From Eq. (28), the elements of $(\mathbf{L}'_i + s_i)^{-1}$ obviously do not exceed $1/s_i$ in absolute value, and because $s_i \geq k_{i1}$, the weak minor exchange condition (32) implies that the off-diagonal elements in Eq. (33) are significantly smaller than 1. In the zero-order approximation $\bar{z}_i = \bar{z}'_i$, as in the case of no minor exchange, while the next order of approximation uses the expansion $(\mathbf{1} + \epsilon \mathbf{X})^{-1} \approx \mathbf{1} - \epsilon \mathbf{X}$:

$$\bar{z}_i \approx \bar{z}'_i + \sum_{\substack{j \geq 2 \\ j \neq i}} k_{ij}(\mathbf{L}'_i + s_i)^{-1} \bar{z}'_j. \quad (34)$$

Combining this result with Eqs. (26) and (30) yields:

$$R_{1\rho} = \cos^2 \theta_1 R_{11} + \sin^2 \theta_1 R_{21} + \sin^2 \theta_1 \left[\sum_{i=2}^n \frac{k_{1i}}{s_i^2 + \omega_{e_i}^2} \times \left[\Delta \omega_{i1}^2 + \frac{1}{s_i} \sum_{\substack{j=2 \\ j \neq i}}^n \frac{k_{ij} \Delta \omega_{j1}}{s_j^2 + \omega_{e_j}^2} + ((\omega^2 + \delta_1 \delta_i) \Delta \omega_{ji} + s_i^2 \Delta \omega_{j1} + s_i s_j \Delta \omega_{i1}) \right] \right]. \quad (35)$$

Fig. 2 illustrates this expression for a 3-site exchange process. The effect of weak minor exchange increases the exchange broadening compared to results obtained in the absence of minor exchange.

3.3. Population-averaged values

Let us introduce the population-averaged values:

$$\delta = \sum_{i=1}^n p_i \delta_i, \quad (36)$$

$$\omega_e = \sqrt{\delta^2 + \omega^2}, \quad (37)$$

$$\sin \theta = \omega / \omega_e, \quad (38)$$

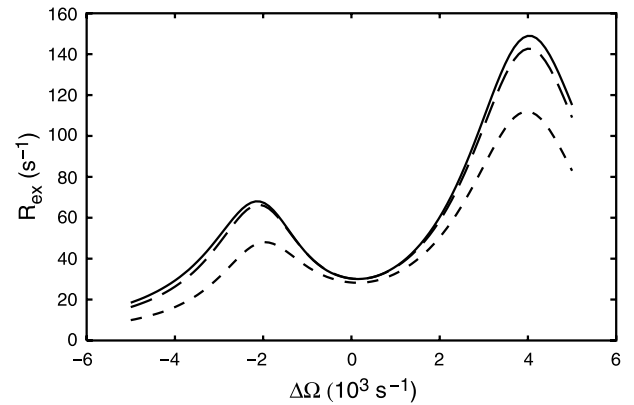


Fig. 2. Offset dependence of R_{ex} for a system with weak minor exchange. The solid line represents the exact numerical solution and the dashed and dotted lines show the approximate solutions obtained from Eqs. (35) and (31), respectively. Calculations used $\omega = 1000 \text{ s}^{-1}$, $p_1 = 0.95$, $p_2 = 0.03$, $p_3 = 0.02$, $\delta_2 - \delta_1 = 2000 \text{ s}^{-1}$, $\delta_3 - \delta_1 = -4000 \text{ s}^{-1}$, $k_{12} + k_{21} = 500 \text{ s}^{-1}$, $k_{13} + k_{31} = 1000 \text{ s}^{-1}$, $k_{23} + k_{32} = 700 \text{ s}^{-1}$, $R_1 = 1.5 \text{ s}^{-1}$, and $R_2 = 11 \text{ s}^{-1}$. The abscissa $\Delta \Omega$ indicates the difference between ω_{rf} and the population-average resonance frequency.

$$\cos \theta = \delta / \omega_e, \quad (39)$$

$$R_1 = \sum_{i=1}^n p_i R_{1i}, \quad (40)$$

$$R_2 = \sum_{i=1}^n p_i R_{2i}. \quad (41)$$

The differences resulting from replacing $\sin \theta_1$, $\cos \theta_1$, R_{11} , and R_{21} with the respective population-averaged values in Eqs. (26), (27), (31), and (35), are second order (quadratic or bilinear) in p_i , R_{1j} , and R_{2j} , where $i = 2, \dots, n$, $j = 1, \dots, n$. Therefore, these differences can be ignored and population-averaged values can be substituted into Eqs. (26), (27), (31), and (35).

4. Free-precession evolution

The above formalism is easily adapted to the free-precession evolution of transverse magnetization in the absence of radiofrequency fields. The resonance line of the dominant component of the complex magnetization, $M^+(t)$, is described by a resonance frequency and a relaxation rate constant given by:

$$i\Omega - R_2 = i\delta_1 - R_{21} + \lambda, \quad (42)$$

in which λ is the eigenvalue of $\mathbf{D} = \mathbf{L} + \mathbf{K}$ with the largest (least negative) real part, $L_i = L'_i = i\Delta \omega_{i1} - \Delta R_{2i}$, and $\Delta R_{2i} = R_{2i} - R_{21}$. For free-precession evolution of transverse magnetization, $\mathbf{1}_s = \mathbf{1}$. The right eigenvector of \mathbf{D}' , corresponding to its zero eigenvalue, is $\vec{x} = (1, 0, \dots, 0)^T$, and by direct analogy to the above derivation of Eq. (26),

$$i\Omega - R_2 = i\delta_1 - R_{21} - \sum_{i=2}^n k_{1i}z_i, \quad (43)$$

in which

$$\begin{pmatrix} s_2 - L_2 & -k_{23} & \cdots & -k_{2n} \\ -k_{32} & s_3 - L_3 & \cdots & -k_{3n} \\ \vdots & \vdots & \ddots & \vdots \\ -k_{n2} & -k_{n3} & \cdots & s_n - L_n \end{pmatrix} \begin{pmatrix} z_2 \\ z_3 \\ \vdots \\ z_n \end{pmatrix} = - \begin{pmatrix} L_2 \\ L_3 \\ \vdots \\ L_n \end{pmatrix}. \quad (44)$$

The resonance frequency and relaxation rate constant are obtained from the imaginary and real parts of the right-hand side of Eq. (43), respectively. Eq. (43) is another of the principal results of this paper.

In the absence of minor exchange,

$$z_i = \frac{-i\Delta\omega_i + \Delta R_{2i}}{k_{i1} - i\Delta\omega_i + \Delta R_{2i}} = \frac{\Delta R_{2i}(k_{i1} + \Delta R_{2i}) + \Delta\omega_i^2 - i\Delta\omega_i k_{i1}}{(k_{i1} + \Delta R_{2i})^2 + \Delta\omega_i^2}, \quad (45)$$

which yields

$$\Omega = \delta_1 + \sum_{i=2}^n \frac{k_{1i}k_{i1}\Delta\omega_i}{(k_{i1} + \Delta R_{2i})^2 + \Delta\omega_i^2}, \quad (46)$$

$$R_2 = R_{21} + \sum_{i=2}^n k_{1i} \frac{\Delta R_{2i}(k_{i1} + \Delta R_{2i}) + \Delta\omega_i^2}{(k_{i1} + \Delta R_{2i})^2 + \Delta\omega_i^2}. \quad (47)$$

These equations extend the results of Skrynnikov et al. [15] for 2-site exchange. The n -site Swift–Connick relationships [11] differ from Eqs. (46) and (47) because ΔR_{2i} is replaced by R_{2i} . The present results are more accurate than the Swift–Connick relationships if ΔR_{2i} are small, but R_{2i} are comparable in magnitude to k_{i1} .

For weak minor exchange,

$$z_i = z'_i + \frac{(s_i + \Delta R_{2i} + i\Delta\omega_i)}{(s_i + \Delta R_{2i})^2 + \Delta\omega_i^2} \sum_{\substack{j=2 \\ j \neq i}}^n k_{ij}z'_j, \quad (48)$$

in which

$$z'_i = \frac{\Delta R_{2i}(s_i + \Delta R_{2i}) + \Delta\omega_i^2 - i\Delta\omega_i s_i}{(s_i + \Delta R_{2i})^2 + \Delta\omega_i^2}. \quad (49)$$

4.1. Three sites

For completeness, we provide below some limiting expressions for the exchange contribution to the transverse relaxation rate constant, $R_{\text{ex}} = R_2 - R_{21}$, for 3-site chemical exchange. For simplicity, $s_i \gg \Delta R_{2i}$ and $\Delta\omega_i \gg \Delta R_{2i}$ are assumed; thus, $\Delta R_{2i} = 0$ can be utilized in Eqs. (43)–(49). The general result is derived from Eq. (43). In the absence of minor exchange,

$$R_{\text{ex}} = \frac{k_{12}\Delta\omega_2^2}{k_{21}^2 + \Delta\omega_2^2} + \frac{k_{13}\Delta\omega_3^2}{k_{31}^2 + \Delta\omega_3^2}. \quad (50)$$

For weak minor exchange,

$$R_{\text{ex}} = \frac{k_{12}\Delta\omega_2^2}{s_2^2 + \Delta\omega_2^2} + \frac{k_{13}\Delta\omega_3^2}{s_3^2 + \Delta\omega_3^2} + \frac{(k_{13}k_{32}\Delta\omega_2 + k_{12}k_{23}\Delta\omega_3)(s_3\Delta\omega_2 + s_2\Delta\omega_3)}{(s_2^2 + \Delta\omega_2^2)(s_3^2 + \Delta\omega_3^2)}. \quad (51)$$

5. Fast exchange within a group of sites

The following applies equally to $R_{1\rho}$ relaxation and free-precession evolution. Herein, we shall use \hat{L}_i to denote either evolution operator for site i .

Removing the restriction that the population of the first site is much greater than the populations of all others, let us assume that molecules in some of the n sites exchange very rapidly among themselves, in some sense. Without loss of generality, let these sites be numbered m through n .

If the exchange rates involving sites m through n approach infinity, then on physical grounds, these $n - m + 1$ sites can be treated as a single effective site. This can be shown by noting that the $(M_m, \dots, M_n)^T$ vector will have a quasi-steady state value that belongs to the null space of the kinetics matrix corresponding to the “fast” reactions, i.e.,

$$M_i = \alpha_i M_f, \quad (52)$$

where

$$\alpha_i = p_i / \sum_{j=m}^n p_j, \quad (53)$$

$$M_f = \sum_{i=m}^n M_i. \quad (54)$$

Adding rows m through n of \mathbf{D} , and using Eqs. (52) and (54) generates the master equation for the new effective system of m sites. The evolution operators \hat{L}_i for sites 1 through $m - 1$ will remain unchanged. The evolution operator for the effective site \hat{L}_f , the new m th site, is the population average:

$$\hat{L}_f = \sum_{i=m}^n \alpha_i \hat{L}_i. \quad (55)$$

Similarly, the rate constants for the reactions “leaving” the effective site are the population-averaged values as well:

$$k_{fj} = \sum_{i=m}^n \alpha_i k_{ij}, \quad \text{where } j < m, \quad (56)$$

while the rate constants for the reactions “entering” the effective site are given by

$$k_{jf} = \sum_{i=m}^n k_{ji}, \quad \text{where } j < m. \quad (57)$$

Establishing the conditions of applicability of these formulas is beyond the scope of this paper. The results describe the asymptotic behavior of the system, and are not necessarily valid approximations when the exchange rates involving sites m through n are merely much greater than other exchange rates, the differences between the resonance frequencies, offsets, etc. To illustrate this point, free-precession evolution of transverse magnetization is considered for 3-site exchange. In the first example, site 1 is dominant, $\delta_1 = 0$, $\delta_2 = -\delta_3 = \delta$, $R_{2i} = 0$, and the chemical kinetics are completely symmetric with regard to sites 2 and 3. Then, treating sites 2 and 3 as one effective site predicts $R_{\text{ex}} = 0$ if k_{23} is large. In contrast, the result obtained using Eq. (43) is:

$$R_{\text{ex}} = \frac{2k_{12}\delta^2}{k_{21}^2 + 2k_{21}k_{23} + \delta^2}. \quad (58)$$

In this case, unless $k_{21}k_{23} \gg \delta^2$, the asymptotic expression is in error by an amount on the order of k_{12} . As a second example, Fig. 3 illustrates the convergence of the free-precession R_2 relaxation rate for a 3-site system to an effective value corresponding to a 2-site system, as the exchange rate between sites 2 and 3 grows, while the site populations and other parameters remain constant. This example differs from the first because the populations of sites 2 and 3 are not equal. In this case, asymptotic behavior requires $k_{23} + k_{32} > 10^6 \text{ s}^{-1}$.

As another example of practical interest, Fig. 4 shows results for $R_{1\rho}$ calculated for a linear 3-site system in which the dominant site 1 exchanges with minor site 2 and site 2 exchanges with minor site 3, but sites 1 and 3

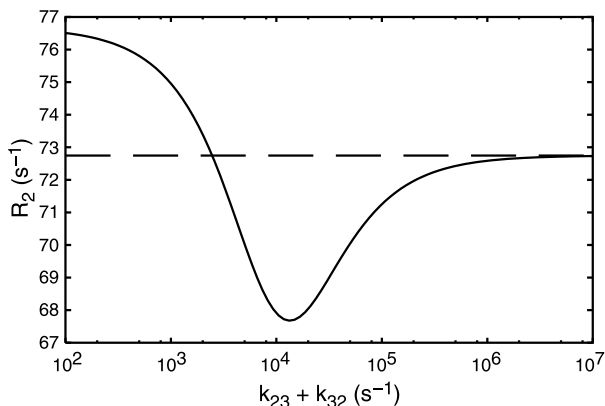


Fig. 3. The dependence of free-precession R_2 on the rate of minor exchange. The solid line represents the exact numerical solution and the dashed line shows the exact solution for the effective 2-site system obtained using Eqs. (55)–(57). Calculations used $p_1 = 0.80$, $p_2 = 0.13$, $p_3 = 0.07$, $\delta_2 - \delta_1 = 3000 \text{ s}^{-1}$, $\delta_3 - \delta_1 = -3000 \text{ s}^{-1}$, $k_{12} + k_{21} = 300 \text{ s}^{-1}$, $k_{13} + k_{31} = 300 \text{ s}^{-1}$, and $R_2 = 11 \text{ s}^{-1}$. The abscissa $k_{23} + k_{32}$ shows the rate of exchange between sites 2 and 3.

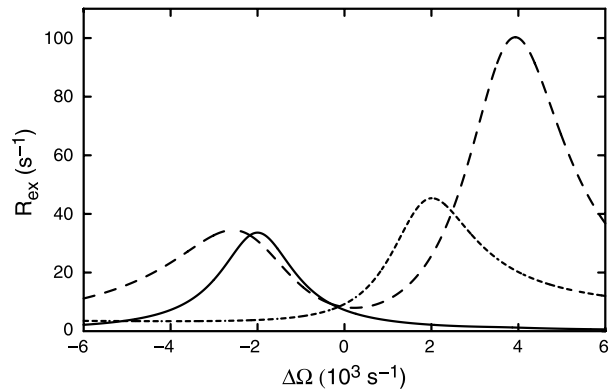


Fig. 4. Offset dependence of R_{ex} for a linear 3-site system. Curves were calculated using Eqs. (26) and (27) for (—) $k_{23} + k_{32} = 1 \text{ s}^{-1}$, (---) $k_{23} + k_{32} = 1000 \text{ s}^{-1}$, and (- · -) $k_{23} + k_{32} = 100,000 \text{ s}^{-1}$. Other parameters used in the calculations were: $\omega = 1000 \text{ s}^{-1}$, $p_1 = 0.94$, $p_2 = 0.02$, $p_3 = 0.04$, $\delta_2 - \delta_1 = 2000 \text{ s}^{-1}$, $\delta_3 - \delta_1 = -4000 \text{ s}^{-1}$, $k_{12} + k_{21} = 500 \text{ s}^{-1}$, $k_{13} + k_{31} = 0 \text{ s}^{-1}$, $R_1 = 1.5 \text{ s}^{-1}$, and $R_2 = 11 \text{ s}^{-1}$. The abscissa $\Delta\Omega$ indicates the difference between ω_{rf} and the population-average resonance frequency.

do not directly exchange. If exchange between sites 2 and 3 is very slow, then a single peak is obtained in the plot of R_{ex} versus $\Delta\Omega$. The system well described by 2-site exchange in which only sites 1 and 2 are considered. If exchange between sites 2 and 3 is comparable to the other rate constants and the chemical shift differences between sites, then two peaks are evident in the plot. If exchange between sites 2 and 3 becomes very fast, then a single peak is observed in the graph because sites 2 and 3 are effectively averaged and the system is described approximately by a 2-site exchange process.

6. Computational fitting experiments

Eq. (31) demonstrates that if minor exchange is absent, the exchange rates are slow, and ω is significantly smaller than any differences among the resonance frequencies, then the local maxima of R_{ex} as a function of the offset occur close to where the rf is resonant with the minor species. From continuity considerations, or from Eq. (35), the same conclusion should apply to systems with weak minor exchange. One result of this paper is that such n -site systems can be studied in a similar fashion to the asymmetric 2-site system, as suggested earlier in [4].

Numerical simulations show that even in situations that may be outside of the weak minor exchange limit, where Eqs. (31) and (35) do not strictly apply, and when the system does not necessarily have a dominant site, a plot of R_{ex} as a function of offset frequency often still exhibits $n - 1$ Lorentzian-shaped peaks.

Therefore, we examined the feasibility of fitting experimental $R_{1\rho}$ measurements in these cases and to develop an algorithm suitable for this task. To this end, we

simulated idealized $R_{1\rho}$ measurements involving a 3-site system in which the rf offsets with respect to the resonance frequency of the first site were taken to be the 30 equidistant points spanning the interval $[-5000, 5000]$, the populations p_1 , p_2 , and p_3 , as well as the intrinsic relaxation rates R_1 and R_2 were assumed known, while the exchange rates and the resonance frequencies were to be inferred from the “experimental” $R_{1\rho}$ relaxation rates. The intrinsic relaxation rate constants can be obtained experimentally by a variety of approaches [16]. In practice the population-averaged resonance frequency, instead of the exact knowledge of the resonance frequency of the first site, and any additional known information about the system would be added as constraints.

The system input parameters were chosen to satisfy the following relationships:

$$\begin{aligned} \omega &= 1000, \\ 0.4 < p_1 < 0.95, \\ 0.02, 0.1(1 - p_1) < p_2 < 0.4(1 - p_1), \\ p_3 &= 1 - p_1 - p_2, \\ 2000 < \delta_2 - \delta_1 < 4000, \\ 2000 < \delta_1 - \delta_3 < 4000, \\ 100 < k_2, k_{sd}, k_3 < (\delta_2 - \delta_1)/3, (\delta_1 - \delta_3)/3, \\ R_1 &= 1.5, \\ R_2 &= 11, \end{aligned} \quad (59)$$

where $k_2 = k_{12} + k_{21}$, $k_3 = k_{13} + k_{31}$, and $k_{sd} = k_{23} + k_{32}$, all frequencies are in angular units, and exchange rate constants and relaxation rate constant are in units of s^{-1} . The inequalities denote the uniform distributions from which the parameters were selected randomly. Because the site populations are known, only the sum of the forward and back exchange rate constants for each pair of sites are required: the individual rate constants can be determined using the detailed balance principle.

Experimentally, only systems with sufficiently low $R_{1\rho}$ values and narrow spectral lines can be studied; therefore, only the systems with the free-precession relaxation rate and the maximum $R_{1\rho}$ values smaller than $100 s^{-1}$ were used, which amounted to 35% of the randomly selected systems.

We used the Levenberg–Marquardt non-linear least-squares fitting algorithm [17] as implemented by the MINPACK optimization package [18] to perform parameter fitting, and the LAPACK library [19] for eigenvalue calculations. Naive application of the Levenberg–Marquardt algorithm showed that the minimization problem is fraught with local minima and is subject to divergence (when one of the unknowns becomes very large). Applying the theoretical insights described in earlier sections, specifically the fact that the local minima of R_{ex} occur close to where the rf is resonant with the minor sites, to the initial choice of un-

Table 1
Computational fitting experiment results

Error (%)	Success rate (%)	Δ^a (s^{-1})
1	99.1	33
3	96.7	99
10	65.7	186

^a Δ is the root mean square deviation from the “true” value.

known variables in the optimization procedure significantly improved its convergence properties.

To simulate the experimental error, random values taken from the Gaussian distribution with the standard deviation calculated as a fraction of the maximum $R_{1\rho}$ value for each system were added to the “experimental” $R_{1\rho}$ values.

For each error magnitude, the computational experiment was repeated 1000 times with randomly selected system parameters, as described above. The fitting was considered successful, when the Euclidean distance in the five-dimensional parameter space between the “true” parameter values and those returned by the fitting procedure was smaller than $300 s^{-1}$. The results are summarized in Table 1. The simulations suggest that experimental characterization of at least 3-site chemical exchange processes in proteins is feasible by $R_{1\rho}$ relaxation dispersion measurements.

7. Discussion and conclusion

Chemical exchange effects in NMR spectroscopy provide powerful approaches for characterizing kinetic processes, including intramolecular conformational changes, ligand binding, and folding of proteins and other biological macromolecules [1]. Herein, new analytic expressions have been presented that generalize existing 2-site theoretical descriptions for the spin relaxation rate constant in the rotating frame, $R_{1\rho}$, and for the transverse relaxation rate constant, R_2 . The new expressions are valid for n -site chemical exchange phenomena whenever one site population is dominant. In particular, systems with one dominant site and sufficiently weak exchange among the minor sites will have $R_{ex}(\omega_{rf})$ relaxation dispersion profiles composed of $n - 1$ Lorentzians, as a general rule. The new results are expected to be generally applicable to the investigation of chemical exchange phenomena in proteins and other biological macromolecules using free-precession and spin-locking techniques.

Acknowledgments

O.T. acknowledges support from National Institutes of Health (NIH) Training Grant T32 DK07328. This work was supported by Grant GM59273 from the

National Institutes of Health awarded to A.G.P. Software written in the course of this research is available from the authors upon request.

References

- [1] A.G. Palmer, C.D. Kroenke, J.P. Loria, Nuclear magnetic resonance methods for quantifying microsecond-to-millisecond motions in biological macromolecules, *Methods Enzymol.* 339 (2001) 204–238.
- [2] D.G. Davis, M.E. Perlman, R.E. London, Direct measurements of the dissociation-rate constant for inhibitor–enzyme complexes via the $T_{1\rho}$ and T_2 (CPMG) methods, *J. Magn. Reson. Ser. B* 104 (1994) 266–275.
- [3] D. Abergel, A.G. Palmer, On the use of the stochastic Liouville equation in NMR: application to $R_{1\rho}$ relaxation in the presence of exchange, *Concepts Magn. Reson. A* 19 (2003) 134–148.
- [4] O. Trott, A.G. Palmer, $R_{1\rho}$ relaxation outside of the fast-exchange limit, *J. Magn. Reson.* 152 (2002) 1–4.
- [5] O. Trott, D. Abergel, A.G. Palmer, An average-magnetisation analysis of $R_{1\rho}$ relaxation outside of the fast-exchange limit, *Mol. Phys.* 101 (2003) 753–763.
- [6] C. Deverell, R.E. Morgan, J.H. Strange, Studies of chemical exchange by nuclear magnetization relaxation in the rotating frame, *Mol. Phys.* 18 (1970) 553–559.
- [7] D.M. Korzhnev, V.Y. Orekhov, F.W. Dahlquist, L.E. Kay, Off-resonance $R_{1\rho}$ relaxation outside of the fast exchange limit: an experimental study of a cavity mutant of T4 lysozyme, *J. Biomol. NMR* 26 (2003) 39–48.
- [8] M.J. Grey, C. Wang, A.G. Palmer, Disulfide bond isomerization in basic pancreatic trypsin inhibitor: multi-site chemical exchange quantified by CPMG relaxation dispersion and chemical shift modeling, *J. Am. Chem. Soc.* 125 (2003) 14324–14335.
- [9] D. Tolkatchev, P. Xu, F. Ni, Probing the kinetic landscape of transient peptide–protein interactions by use of peptide ^{15}N NMR relaxation dispersion spectroscopy: binding of an antithrombin peptide to human prothrombin, *J. Am. Chem. Soc.* 125 (2003) 12432–12442.
- [10] M. Tollinger, N.R. Skrynnikov, F.A.A. Mulder, J.D. Foreman-Kay, L.E. Kay, Slow dynamics in folded and unfolded states of an SH3 domain, *J. Am. Chem. Soc.* 123 (2001) 11341–11352.
- [11] T.J. Swift, R.E. Connick, NMR-relaxation mechanisms of Os^{17} in aqueous solutions of paramagnetic cations and the lifetime of water molecules in the first coordination sphere, *J. Chem. Phys.* 37 (1962) 307–320.
- [12] J. Cavanagh, W.J. Fairbrother, A.G. Palmer, N.J. Skelton, *Protein NMR Spectroscopy*, Academic Press, New York, 1996.
- [13] H.M. McConnell, Reaction rates by nuclear magnetic resonance, *J. Chem. Phys.* 28 (1958) 430–431.
- [14] J.H. Wilkinson, *The Algebraic Eigenvalue Problem*, Clarendon Press, Oxford, 1972.
- [15] N.R. Skrynnikov, F.W. Dahlquist, L.E. Kay, Reconstructing NMR spectra of “invisible” excited protein states using HSQC and HMQC experiments, *J. Am. Chem. Soc.* 124 (2002) 12352–12360.
- [16] A.G. Palmer, NMR characterization of the dynamics of biomacromolecules, *Chem. Rev.* 104 (2004), in press.
- [17] K. Levenberg, A method for the solution of certain non-linear problems in least squares, *Q. J. Appl. Math.* 2 (1944) 164–168.
- [18] J.J. Moré, B.S. Garbow, K.E. Hillstom, User guide for MINPACK-1, Tech. Rep. ANL-80-74, Argonne National Laboratory, Argonne, IL, USA, 1980.
- [19] E. Anderson, Z. Bai, C. Bischof, J. Demmel, J. Dongarra, J. DuCroz, A. Greenbaum, S. Hammarling, A. McKenney, D. Sorensen, LAPACK: a portable linear algebra library for high-performance computers, Tech. Rep., Knoxville, 1990. Available from <citeseer.ist.psu.edu/anderson90lapack.html>.